4ICEGE Thessaloniki-GREECE 2007

4th International Conference on
Earthquake Geotechnical Engineering
June 25-28, 2007
Paper No. 1213

EMBEDDED INSTRUMENTATION FOR COUPLED SHEAR STRAIN-PORE PRESSURE RESPONSE IN MULTIDIRECTIONAL SHAKING TABLE TEST

Wen-Jong CHANG[1], Tzou-Shin UENG[2], Chia-Han CHEN[3], and Chih-Wei YANG[4]

ABSTRACT

A new instrumentation system was developed and implemented on a biaxial laminar shear box for modeling the free-field response. The main purpose of the instrumentation is to measure the coupled shear strain-pore pressure response of saturated sands subjected to multidirectional shaking. A low-frequency triaxial accelerometer and a miniature piezometer were integrated in a small case to measure the local particle motions and pore pressure variations. Four integrated sensors were deployed to form a square instrumentation array on the plane parallel to the wave propagation direction. Embedded sensors were installed during the sample preparation stage and were acquired by a high-speed data acquisition system capable of synchronizing with other instrumentation system. Four shear strain evaluation methods, which use either the particle displacements or the particle velocities computed by integrating the acceleration data numerically, were implemented to calculate the shear strain time-histories at locations with simultaneous pore pressure measurements. In addition, relative displacements of box frames were used to calculate average shear strains of soils confined between frames. Series of shaking table tests with different acceleration amplitudes, frequencies, durations, and shaking directions were performed on a saturated clean sand. Comparisons among shear strains evaluated by embedded sensors and relative displacements of frames are conducted to verify the performance of the embedded instrumentation and to assess the boundary effects of the laminar shear box. Coupled shear strain-pore pressure behaviors in liquefied and nonliquefied cases are presented and discussed. More insights of the interactions between the induced shear strain and generated excess pore pressure are shown.

Keywords: Liquefaction, Shaking Table Test, Laminar Shear Box, Shear Strain Evaluation, Coupled Response

INTRODUCTION

Soil liquefaction is a coupled response between the induced shear strain and the generated excess pore pressure. The field temporal and spatial variations of excess pore pressure could be affected by several factors, such as upward seepages (Yoshimi & Kuwabara 1973), formation of a water film (Kokusho & Kojima 2002), stratified soil effects (Amini & Sama 1999), and alternations of ground motions. Therefore, local and simultaneous measurements of the induced shear strains due to upward propagating shear waves and the generated excess pore pressures are necessary to enhance the understating of soil liquefaction.

[1] Assistant Professor, Department of Civil Engineering, National Chi Nan University, Puli, Taiwan, Email: wjchang@ncnu.edu.tw
[2] Professor, Department of Civil Engineering, National Taiwan University, Taipei, Taiwan.
[3] Assistant Research Fellow, National Center for Research on Earthquake Engineering, Taipei, Taiwan.
[4] Former Graduate Student, National Chi Nan University, Puli, Taiwan.

Using large soil specimens attached on a shaking table to physically model seismic responses of soils has been an important branch in the field of geotechnical earthquake engineering. Advantages of using large specimens include less boundary effects, more accurate to mimic the field stress conditions prior and during the seismic loading, feasible to measure responses at different locations, and less disturbances from the installed instrumentations. These features will be crucial in liquefaction study.

To conduct liquefaction tests on a shaking table requires a model container to simulate the free-field responses of soil deposits and to contain the testing materials. Conventionally, laminar shear boxes have been used to represent the free-field condition in a limited size specimen. The container-soil interfaces impose boundary conditions that do not exist in the prototype condition. The boundary effects raise concerns regarding the shear strains evaluated from relative displacements of the container. Factors affecting the accuracy of strain evaluations include the consistence of specimen deformations, deformation modes, frame rigidity, and interface interactions. In addition, pore pressures and shear strains measured at different locations can not precisely capturer the coupled responses due to time lag.

This paper presents a new instrumentation system developed to locally monitor the coupled shear strain-pore pressure behaviors of saturated sands subjected to horizontal shaking. The instrumentation was implemented to a bidirectional laminar shear box to simulate liquefaction in free-field conditions. The framework of the instrumentation system, data reduction procedures, and preliminary testing results on a clean sand are presented here. The coupled shear strain-pore pressure behaviors in liquefied and nonliquefied cases are presented and discussed as well.

FACILITIES AND TESTING CONDITIONS

Shaking table and laminar shear box

The flexible laminar shear box used in this research was developed at National Center for Research on Earthquake Engineering (NCREE) and was placed on the multidirectional shaking table at the same institute. The laminar shear box is consisted of 15 layers of light-weight aluminum alloy frame with a specimen size of 1.88 by 1.88 by 1.52 m in length, width, and height respectively. Each layer of the frame is composed of two nested frames supported independently on the outside rigid wall, as shown schematically in Figure 1. Each frame is 80 mm in height with 20 mm gap between layers except the top frame, which is 100 mm high. Key features of the NCREE laminar shear box include: (1) capability of bidirectional shaking on the horizontal plane without producing torsion, (2) no accumulation of both frictional and inertial effects of frames, and (3) tolerance of large relative motions between layers. The performances of the NCREE laminar shear box had been critical verified and the unique design of the laminar shear box could well model the free-field responses subjected to upward propagating shear waves (Ueng et al. 2006).

Instrumentation system

Highly dense instrumentation was installed both inside and outside the soil specimen to measure the soil motions, pore pressure variations, and frame movements. Details are provided as followings.

Coupled sensor

Composed sensor, which integrates a 3-axis low-frequency accelerometer and a miniature pore pressure transducer in an acrylic case, was fabricated as shown in Figure 2. The coupled sensor is the modified version of Chang (2002). To fit the frequency range in the shaking table tests, a 3-axis capacitive accelerometer manufactured by PCB is integrated with a miniature pore pressure transducer by Druck. The composed sensors are called coupled sensor to reflect their design purposes. These coupled sensors are relatively small (12 cm long, 5.5 cm in diameter) enabling them to simultaneously measure both the particle accelerations and pore pressure at almost the same location. Four sensors were deployed to form a 0.6 m by 0.6 m square array on the vertical plane parallel to the wave propagation direction (Figure 3(a)). The square array was used to calculate the shear strain within

the array. The calculated shear strains and recorded pore pressures at various locations could provide insight information of coupled shear strain-pore pressure responses.

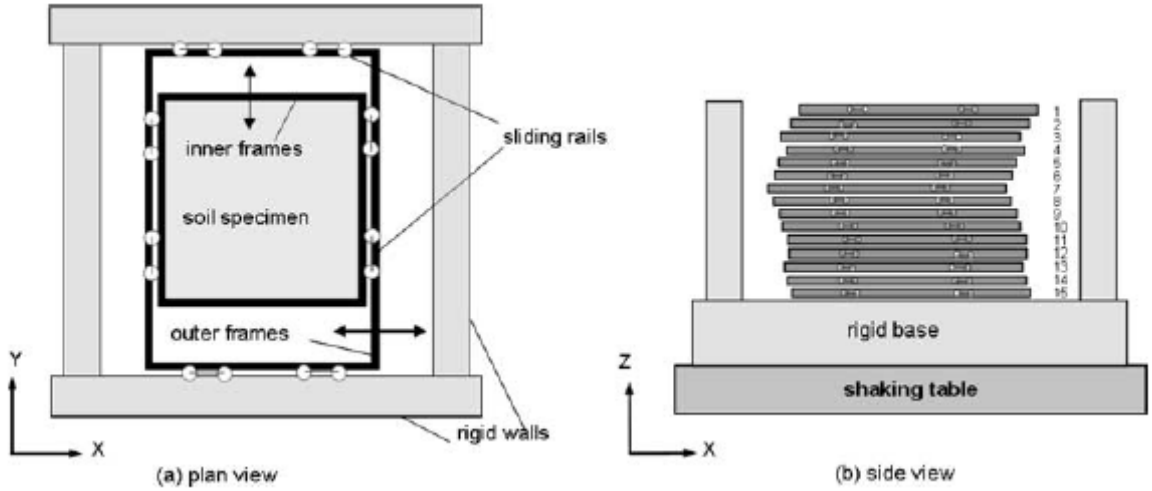

Figure 1. Schematically drawing of biaxial laminar shear box at NCREE (Ueng et al. 2006)

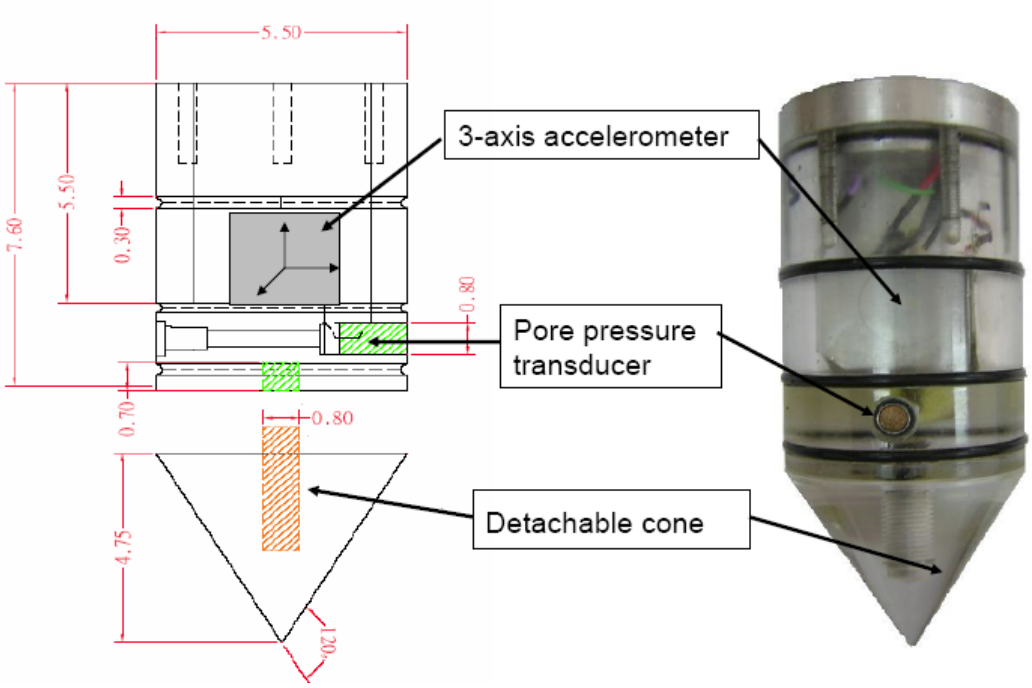

Figure 2. Details of coupled sensor

Internal and external instrumentation systems

In addition to coupled sensors, accelerometers and pore pressure transducers (piezometers) were also embedded in soil specimens to monitor soil motions and pore pressure variations respectively. The configuration of the internal instrumentation is shown in Figure 3(a). Miniature accelerometers (marked as pcb1~4) were evenly placed at the symmetric axis of specimens to measure the horizontal accelerations at different depths. Pore pressure transducers (marked as wp1~15) were installed at different depths of the diagonal plane, as shown in Figure 3(a). These spread pore pressure transducers were used to catch the spatial variations of excess pore pressures. Four coupled sensors were deployed to form an instrumentation array for various strain evaluation techniques. Outside the specimen, magnetostriction-type linear displacement transducers (LDTs) and accelerometers were used to measure the horizontal displacements and accelerations of each frame respectively, as shown

in Figure 3(b). On the rigid wall and the base of the shaking table, horizontal accelerometers were used to record the acceleration of the rigid wall and the base acceleration. These sensors inside specimen and on model container could provide data for cross comparisons of different shear strain evaluation methods and close observations of the coupled responses.

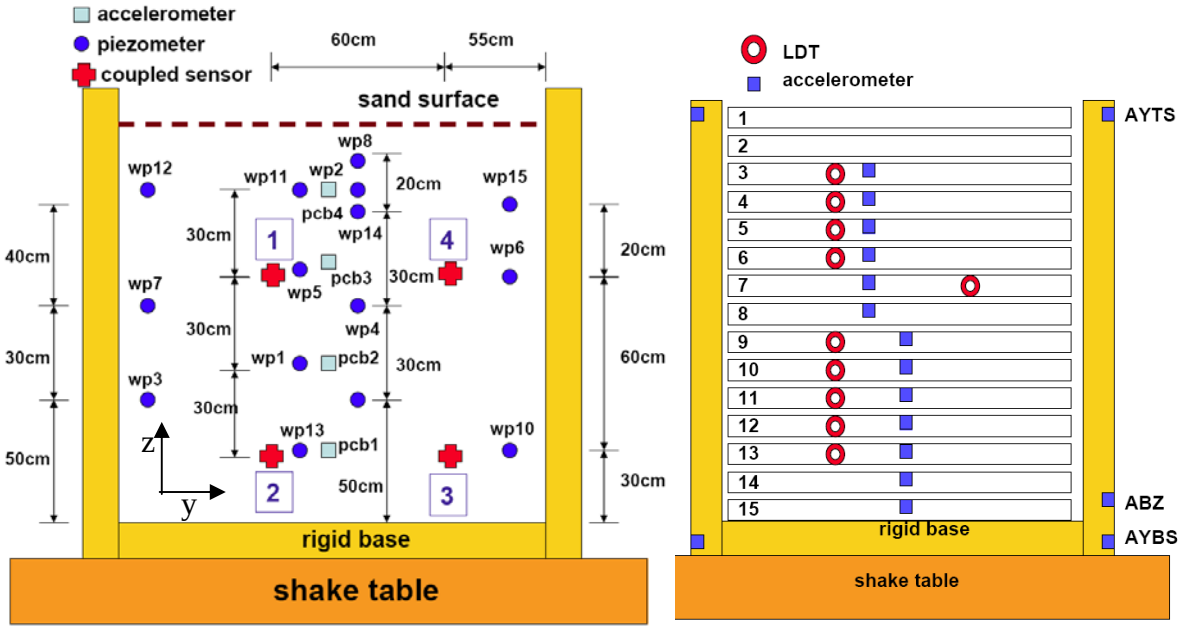

(a)

(b)

Figure 3. Cross sections of instrumentation system (a) internal (b) external

Data acquisition systems

Most sensors were connected to the data acquisition system at NCREE except the four coupled sensors, which were acquired by a stand-alone, customized high-speed data acquisition system with high sampling rate and easy expansion. To synchronize the two data acquisition systems, the accelerometer on the base of the shaking table were connected to both systems and used as the reference channel. Synchronization was performed after testing based on the time difference of the reference channel between the two systems.

Testing material and sample preparation

The testing material is a fine silica sand from Vietnam, which had been used in various liquefaction studies in Taiwan for its consistent gradation and easy purchasing. The Vietnam sand is white in color with a specific gravity of 2.65, maximum void ratio of 0.92, and minimum void ratio of 0.61. The USCS classification of the Vietnam sand is poor graded sand (SP).

Saturated specimens were prepared in water sedimentation fashion with a pluviator hanging above the laminar shear box. The sample preparation procedure used in this study had been verified to produce saturated, uniform specimens with initial dry density ranging from 1440 kg/cm^3 to 1490 kg/cm^3, depending on the rate of pluviation (Ueng et al. 2006).

Testing program

A series of shaking table tests had been performed on the sand specimen in August 2005. Various input motions were generated by the shaking table. There were 32 tests conducted, including sinusoidal accelerations in one direction with acceleration amplitudes ranging from 0.01 g to 0.2 g, frequency from 1 to 8 Hz, and durations from 4 to 11 seconds. Bidirectional motions in the horizontal direction were also conducted with 90-defree phase difference between the two horizontally orthogonal directions. In addition, the Kobe earthquake record scaled to 0.2 g was performed to

study the effects of irregular input motion. In this paper, only the sinusoidal inputs in one direction are discussed.

DATA REDUCTION

Data reduction procedures

The recorded data include acceleration and pore pressure time histories of the soil specimen and the acceleration and displacement time histories of frames. Soil accelerations and frame movements were processed to calculate shear strains. Pore pressure data were processed to highlight characteristics during and after the shaking. Coupled behaviors of liquefied sands can be observed from the shear strain and pore pressure data at same location.

Shear strain evaluation techniques

Four shear strain evaluation techniques are used in current study. They are categorized as displacement-based and wave propagation-based methods. The displacement-based methods use the relative displacements between different locations. Three displacement-based methods are used in current stage, including 2D and 1D displacement-based methods and a shear beam method. The wave propagation-based method is based on plane shear wave propagation characteristics. A plane shear wave method is adopted in current study. Summary of the four methods are tabulated in Table 1 and details are provided in following paragraphs.

2D displacement-based method

The 2D displacement-based method (denoted as 2DBM) uses the same technology described by Rathje et al. (2005). The instrumentation array formed by four coupled sensors is considered as a 4-node element with 2 degrees of freedoms (vertical and horizontal) per node. The vertical and horizontal directions are parallel to the wave propagating direction (i.e., z-direction) and the particle motion direction (i.e., y-direction) respectively. Adopting the displacement approach in the finite element method, strain components within the element can be linearly interpolated from the 8 nodal displacement components (2 components per node). Assume the element size in Figure 3(a) is 2*a* by 2*a* and the origin (y=0, z=0) of the element is at the center of the array. The shear strain of any point within the element with coordinates y and z is expressed as:

$$\gamma_{yz}(y,z)=\frac{1}{4}\left[\frac{u_{y1}}{a}(1-y/a)-\frac{u_{z1}}{a}(1+\frac{z}{a})-\frac{u_{y2}}{a}(1-\frac{y}{a})-\frac{u_{z2}}{a}(1-\frac{z}{a})\right.$$
$$\left.-\frac{u_{y3}}{a}(1+\frac{y}{a})+\frac{u_{z3}}{a}(1-\frac{z}{a})+\frac{u_{y4}}{a}(1+\frac{y}{a})+\frac{u_{z4}}{a}(1+\frac{z}{a})\right] \quad (1)$$

where u_{ij} is the displacement in the i direction (i = y or z) at node j (j = 1 to 4). The nodal displacement components are computed by numerically integrating the vertical and horizontal acceleration records.

The most critical assumption employed in this strain formulation is the linear variation of displacements between nodes. To satisfy this assumption, wavelengths of waves traveling through the instrumentation array should be much larger than the array size. To ensure that the computed strains are not significantly affected by the assumption, it is recommended that the largest dimension of the instrumentation array be smaller than 1/5 of the wavelength. In the following discussions, the 2DBM is used as the reference method in comparing with others because of fewer assumptions.

Shear beam and 1D displacement-based methods

In a 1D shear wave propagation condition, a soil deposit can be modelled as a stack of shear beams and the average shear strain between two depths (γ_{12}) is defined as:

$$\gamma_{12}=\frac{u_{y1}-u_{y2}}{(z_2-z_1)} \quad (2)$$

where u_{yi} represents the horizontal displacement of point *i* at depth of z_i. Alternatively, the shear beam method is identical to the 1D form of Equation (1). To match the shear beam assumptions, only horizontal displacements are allowed and horizontal displacements at same depth are the same. In other words, displacements in the z-direction are zero and displacements in the y-direction satisfy $u_{y1}=u_{y4}$ and $u_{y2}=u_{y3}$. The average shear strain between sensor 1 and 2 is reduced to:

$$\gamma_{12} = \frac{u_{y1} - u_{y2}}{2a} \tag{3}$$

Equation (3) is identical to equation (2). In shaking table tests, the horizontal displacements are from double integrations of accelerations measured by embedded accelerometers or direct measurements of frame movements by LDTs. The shear beam method using the embedded sensors is named the 1D displacement-based method (denoted as 1DBM) and the other is named the frame shear beam method (denoted as FSBM). Differences between two methods depend on the significance of boundary effects and will be compared and discussed later.

Plane shear waves method

The plane shear wave method (denoted as PSWM) is one of the wave-propagation methods, which utilizes the particle velocity and wave propagation velocity to compute strain components (Richart et al., 1970). The plane shear wave method assumes only one-dimensional shear waves traveling through the specimen. In current testing configuration, upward propagating shear waves are generated and propagating at a wave velocity of V_s. The shear strain at a specific point is evaluated by:

$$\gamma_{yz} = \frac{\dot{u}_y}{V_s} \tag{4}$$

where $\dot{u}_y$ is the horizontal particle velocity. Assuming that the wave velocity is constant during the entire testing process, the wave velocity measured before shaking can be used to compute strains. It is noteworthy that this assumption might be not valid for cases with varied shear wave velocities (e.g., liquefaction, site response under high levels of shaking) and could cause significant errors.

Pore pressure processing

The miniature pore pressure transducer in coupled sensors recorded pore pressure-time history. The recorded pore pressure contained three components: (a) the hydrostatic pore pressure of the water table, (b) the hydrodynamic pore pressure oscillating with the dynamic loading, and (c) the residual pore pressure representing the accumulations and dissipations of excess pore pressure. In liquefaction study, the hydrostatic component is less important and is subtracted from the records first. Consequently, only the excess pore water pressure is processed. To highlight and analyze the hydrodynamic and residual pore pressures separately, band-pass and low-pass filters are used respectively. A band-pass filter removes signals components with frequencies outside the specified frequency band. A low-pass filter removes signals components with frequencies above a specified frequency called cutoff frequency.

TESTING RESULTS AND DISCUSSIONS

Verifications of system compliance

In current configuration, two instrumentation systems were used and both systems were synchronized with a reference channel. To verify the system compliance between different systems, sensors acquired by two data acquisition systems are presented and shown in Figure 4. The input motion in Figure 4 is a 1D horizontal acceleration at Y-direction with the maximum acceleration of 0.05 g at

Table 1. Summary of shear strain evaluation methods

Method (acronym)	Fundamental relationship	Measured properties	Calculation properties	Prior Information
2D displacement-based method (2DBM)	Equation (1)	Nodal displacements at 4 nodal points	Strain components at points inside array	None
1D displacement-based method (1DBM)	Equation (3)	Horizontal displacements at 2 internal points	Average shear strain between two elevations	None
Frame shear beam method (FSBM)	Equation (2)	Horizontal displacements of 2 frames	Average shear strain between two frames	None
Plane shear wave method (PSWM)	Equation (4)	Horizontal particle velocity at measured point	Shear strain at measured location	Shear wave velocity

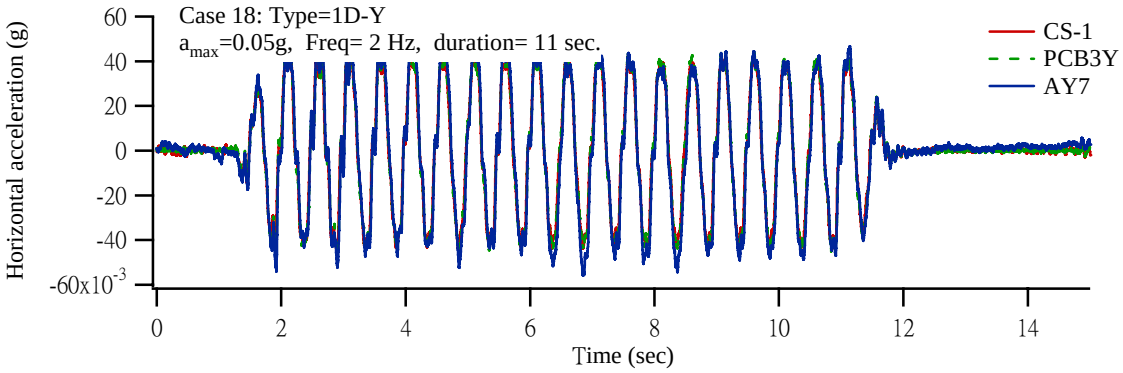

(a)

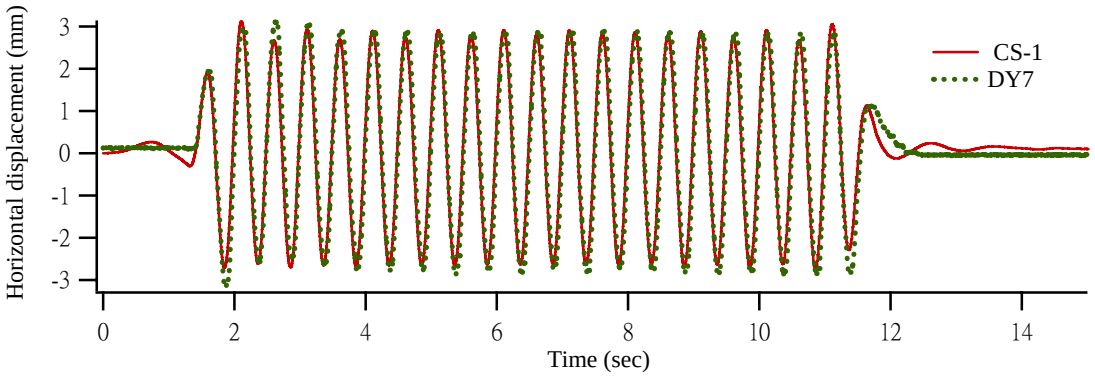

(b)

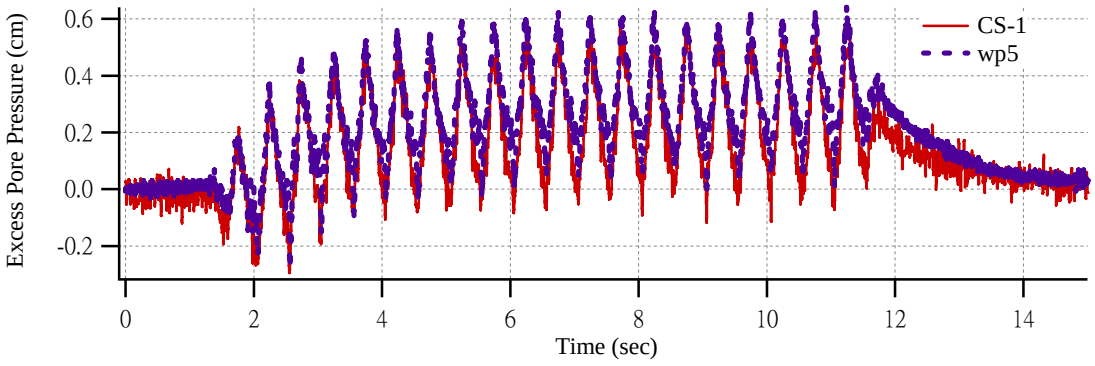

(c)

Figure 4. Verifications of system compliance (a) acceleration, (b) displacement, and (c) excess pore pressure

frequency of 2 Hz for 11 seconds. Figure 4(a) shows the accelerations of coupled sensor 1 (CS-1) and PCB3Y along with the frame acceleration at same elevation (AY7). The results show that the acceleration measurements between two systems are almost identical.

Figure 4(b) shows the horizontal displacement of frame No. 7 in Figure 3(b) (DY7) and the double integration of acceleration at CS-1. Again, the two records are highly matched. Figure 4(c) shows the generated excess pore pressures from CS-1 and wp5, which are at almost the same elevation. The abovementioned results evidently show that the two systems are highly compatible with respect to both the motion and pore pressure measurements.

Shear strain responses of nonliquefied cases

Figure 4 is the typical responses of nonliquefied cases. The induced shear strains evaluated by four methods are plotted together in Figure 5. Because 1DBM , PSWM, and FSBM methods all calculate the average shear strain between two elevations, the shear strain at the middle point of sensor 1 and 2 is calculated in 2DBM for fair comparisons. In all nonliquefied cases, a relatively constant shear strain amplitude was observed throughout the shaking. Shear strains evaluated from embedded coupled sensors (i.e., 2DBM, 1DBM, and PSWM) agreed very well; however, the shear strain evaluated from the relative displacement between frames 7 and 13 showed phase and amplitude differences from the 2DBM data. Although the induced shear strain level exceeded the threshold shear strain of soils, only limited residual pore pressure was generated. The excess pore pressure records in Figure 4(c) represented the state of balance between the generated and dissipating pore pressures.

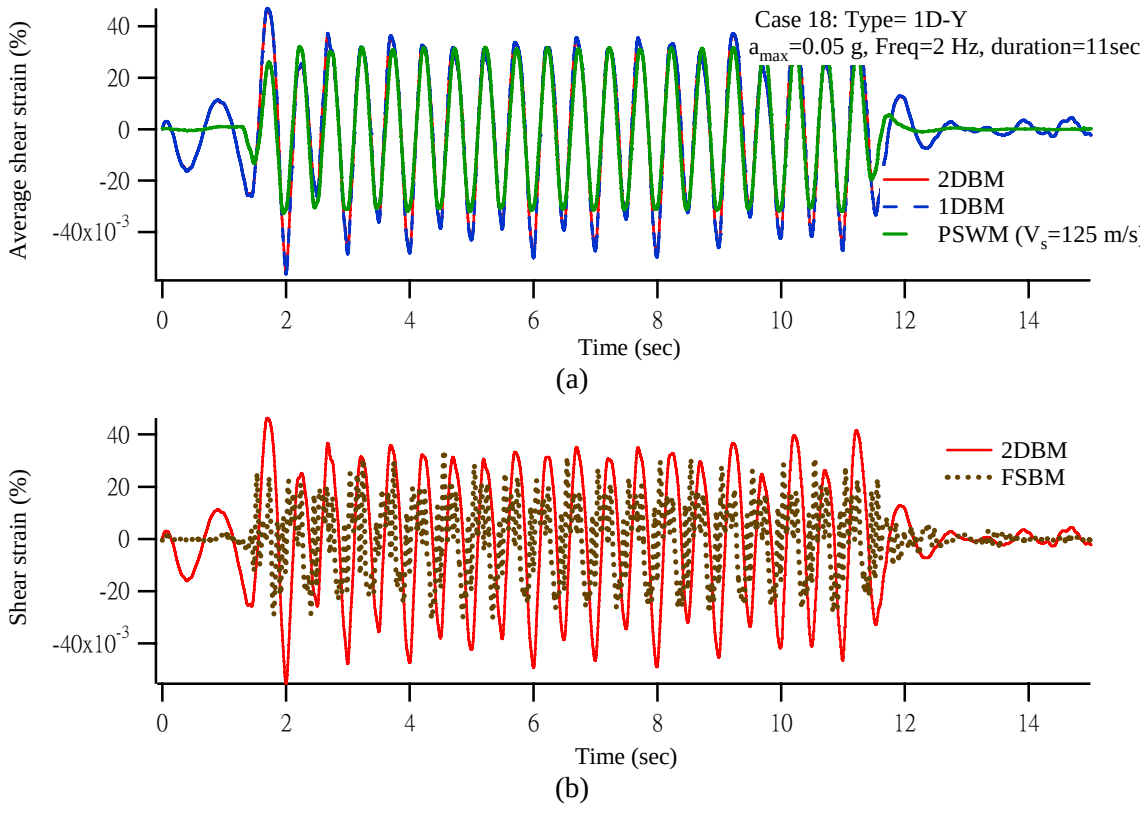

Figure 5. Average shear strain-time histories of a nonliqufied case : (a) shear strains evaluated by coupled sensors (b) comparisons between 2DBM and FSBM

Shear strain responses of liquefied cases

The typical soil responses and variations of excess pore pressure in liquefied cases are shown in Figure 6. The horizontal accelerations of the soil specimen and the frame at same elevation are shown in

Figure 6(a). In contrast with nonliquefied cases, significant differences occurred between the soil and frame after the initiation of liquefaction (i.e., t=2.75 sec). High frequency vibrations were observed on frame, as shown in Figure 6(a).

The displacements of the specimen (CS-1) and the movement on the frame (DY-7) were also different, as shown in Figure 6(b). The recorded frame displacements showed significant permanent displacement was induced in liquefied cases. The filtered displacement in Figure 6(b) represents the oscillation component of the displacement on the frame. The reduction of displacement amplitudes after liquefaction indicated that an energy barrier had been generated around the measured elevation. However, the reason that caused one way permanent displacement instead of a oscillating pattern under sinusoidal shaking needs further investigations.

The strain-time histories at the middle point of sensor 1 and 2 by different strain evaluation methods are shown in Figure 6(c) and the results show that the shear strain by 1DBM are almost identical with the 2DBM ones. The processed data also show that the strain levels by PSWM and FSBM are much smaller than the strain level by 2DBM. Because the displacements induced in sensor 1 were significantly reduced after the initiation of liquefaction (Figure 6(b)), the strains by 2DBM were most contributed by sensor 2 locating in the nonliquefied zone. Therefore, the discrepancies were due to the violation of the linear variation assumption. To improve this, the element size will be reduced next time to make the whole array within the liquefied zone.

Residual excess pore pressures during shaking come from two sources: the excess pore pressure generated by the induced cyclic shear strains of the soil element and the contributions of surrounding soils. The first ones occurred only during the shaking and the induced shear strains should exceed the threshold shear strain level ($\gamma_t \approx 1\times10^{-2}\%$) to generate significant excess pore pressures. However, in cases that the excess pore pressures contributed from surrounding soils were large enough to trigger or maintain the liquefaction state, the induced shear strain level would be unnecessary or irreverent. The excess pore pressure history of sensor 1 (Figure 6(d)) showed that the duration of liquefaction was much longer than the shaking duration. The excess pore pressure-time history of sensor 2, which is 0.6 m deeper than sensor 1, was plotted together with the record of sensor 1. The two records revealed that a specific head difference (15 cm in Figure 6(d)) existed between the 2 sensors at both the start and end of liquefaction state. Because the source of residual pore pressure after shaking was solely from surrounding soils, the pressure distribution in soil deposit could alter the duration of liquefaction.

Numerical studies have been in progress to investigate the strain variations after liquefaction. The results will be benefit to clarify which method is more appropriate in liquefaction study. Also, analytical works to explain the liquefaction state due to pressure distribution in soil deposit are under development.

Comparisons of strain evaluation methods

Average shear strain levels, which represented the average shear strain amplitudes during the loading period, by different strain evaluation methods under various shaking levels for a specific number of loading cycles (n=20~22 cycles) were compiled and shown in Figure 7. As abovementioned, the 2DBM method was used as the reference method for fewer assumptions. The comparisons reveal that all methods agree well for cases with shear strain level less than 2×10^{-2} %. The shear strain levels by FSBM differ from others for cases with strain level exceeding that value. Significant discrepancy exists between the data by 2DBM and PSWM whenever the shear strain level exceeds 4×10^{-2} %. Nevertheless, strain levels by 1DBM and 2DBM agree very well within the induced strain range. It should be noted that these comparisons only valid for 1D wave propagation cases and the 2D effects, which calculate the shear strain from 4 nodal points, are not compared. The effects of vertical components and lateral variations of the induced shear strain will be presented in the near future.

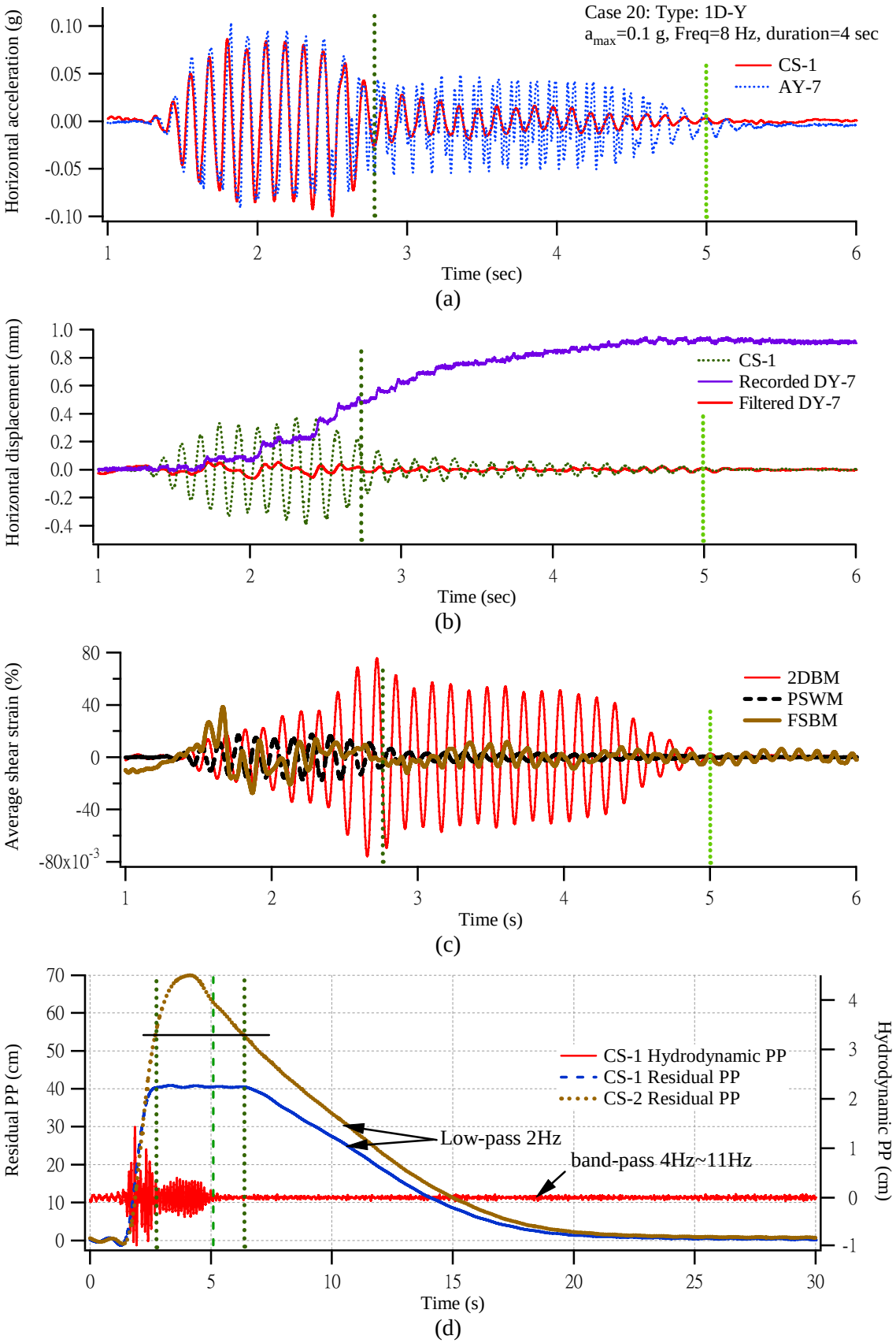

Figure 6. Responses of liquefied cases (a) internal accelerations, (b) displacements, (c) shear strains, and (d) excess pore pressures

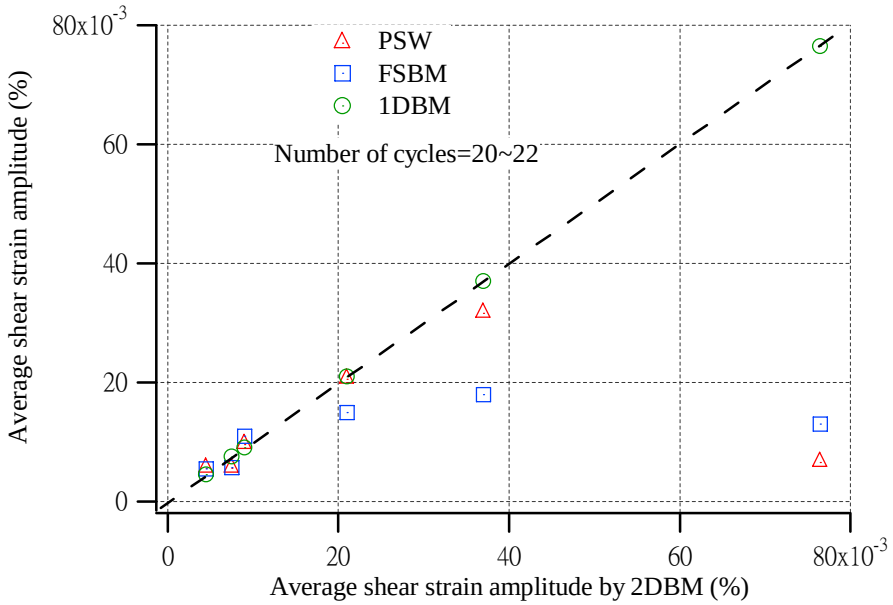

Figure 7. Comparisons of strain evaluation methods

Coupled responses of liquefaction

The major advantage of the new instrumentation system is to measure the local, coupled responses between the induced shear strain and the generated excess pore pressure without time lag. The time histories of excess pore pressure ratio ($r_u = \Delta u / \sigma_v^{'}$, where Δu =excess pore pressure and $\sigma_v^{'}$ =effective vertical stress) and the computed shear strain by 2DBM at the location of sensor 1 are shown in Figure 8. In view of the variations of r_u, the liquefaction process could be divided into different stages. In the first stage, significant excess pore pressure was generated and accumulated. The shear strain levels increased as r_u increased due to reduction of shear modulus. In the second stage, the soil reached initial liquefaction and maintained the liquefaction state until the end of shaking. In this stage, the amplitude of the hydrodynamic excess pore pressure was relatively constant and the shear strain started to decrease. The following stage represented the liquefaction contributed solely by the surrounding soils. It should be addressed that this stage only existed in some liquefied cases. In cases with shallow liquefaction zone, this stage was relatively short or not reached. The final stage represented the dissipation of excess pore pressure.

These coupled characteristics can only be observed in large scale tests and are more representative to the field conditions. The implementations and significances of these features in engineering design need further clarifications.

CONCLUSIONS

This paper presents an on-going research in developing embedded instrumentation to improve the measurements of coupled shear strain-pore pressure responses. Coupled sensors, which integrate a 3-axis accelerometers and a miniature pore pressure transducer in a small case, are used and deployed in a square instrumentation array. Four strain evaluation methods were utilized to evaluate shear strain time-histories in 1D shaking cases. The shear strains by four methods agree well in nonliquefied cases but show significant deviation in liquefied cases. The duration of liquefaction state depends both on the generation of excess pore pressure by the soil element and the distribution of excess pore pressures in the soil deposit. Coupled shear strain-pore pressure responses are demonstrated with the processed pore pressure ratio and the shear strain evaluated at the sensors location by a displacement-based method. According to the variations of the excess pore pressure ratio, liquefaction process is divided into different stages.

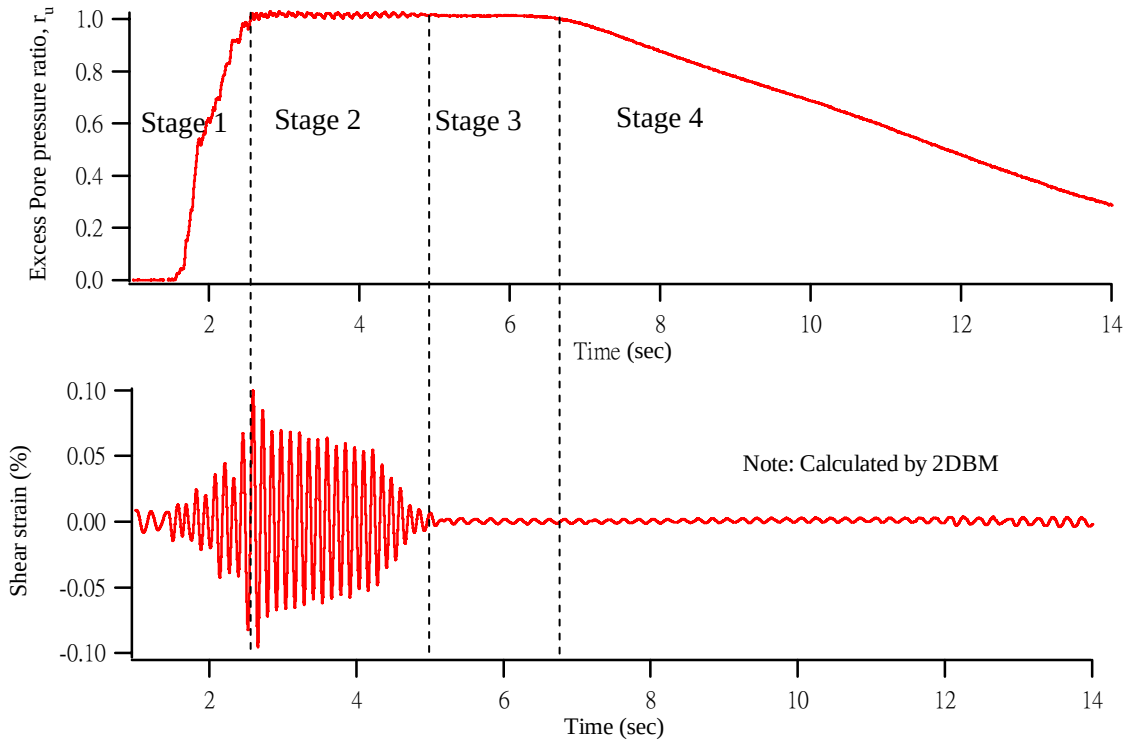

Figure 8. Coupled response of a liquefied case at the location of coupled sensor 1

AKNOWLEDGEMENTS

This study was supported by National Science Council, Taiwan, ROC, under Grant No. NSC 94-2211-E-260-006. The authors would like to express sincere appreciations to engineers at NCREE for their kind assistances in conducting tests on the shaking table.

REFERENCES

Amini F and Sama KM. “Behavior of Stratified sand-silt-gravel composites under seismic liquefaction conditions,” Soil Dynamics and Earthquake Engineering, Vol. 18, 445-455, 1999

Chang WJ. “Development of an In Situ Dynamic Liquefaction Test” Ph.D. Dissertation, University of Texas at Austin, 313 pp, 2002

Kokusho T and Kojima T. “Mechanism for postliquefaction water film generation in layered sand,” Journal of Geotechnical and Geoenvironmental Engineering, ASCE, 128, 2, 129-137, 2002

Rathje EM, Chang WJ, and Stokoe KHII. “Development of an in situ dynamic liquefaction test,” ASTM Geotechnical Testing Journal, 28, No. 1, 65-76, 2005

Richart FE, Hall JR, and Woods RD. Vibration of Soils and Foundations, Prentice-Hall, Inc., New Jersey, 1970

Ueng TS, Wang MH, Chen MH, Chen CH, and Peng LH. “A large biaxial shear box for shaking table test on saturated sand,” Geotechnical Testing Journal, ASTM, 29, No.1, 1-8, 2006

Yoshimi Y and Kuwabara F. "Effects of subsurface liquefaction on the strength of surface soil," Soils and Foundations, JSSMFE, 13, 2, 67-81, 1973